Discontinuous Volume Transitions in Cross-Linked Polyelectrolyte Gels Induced by Short-Range Attractions and Strong Electrostatic Coupling

ARTICLE *in* MACROMOLECULES · APRIL 2004

Impact Factor: 5.8 · DOI: 10.1021/ma035512n

2 AUTHORS, INCLUDING:

Stefanie Schneider
RWTH Aachen University
13 PUBLICATIONS **354** CITATIONS

Discontinuous Volume Transitions in Cross-Linked Polyelectrolyte Gels Induced by Short-Range Attractions and Strong Electrostatic Coupling

Stefanie Schneider* and Per Linse

Physical Chemistry 1, Center for Chemistry and Chemical Engineering, Lund University, P. O. Box 124, S-22100 Lund, Sweden

Received October 7, 2003; Revised Manuscript Received March 3, 2004

ABSTRACT: The swelling behavior of polyelectrolyte gels with and without short-range attraction was studied at variable permittivities using Monte Carlo simulations. The primitive model, with explicit treatment of all charged species augmented with an attractive square-well potential between network particles, was used. Discontinuous volume transitions appeared at critical values of the depth of the square-well potential at fixed permittivity and at critical values of the permittivity at fixed short-range potential. In particular, we observed such a transition also without the short-range potential. The collapsed state was favored by the short-range attraction and/or at low permittivity. The volumes of the collapsed states were 1−2 orders of magnitude smaller than those of the swollen states.

1. Introduction

Polyelectrolyte gels are of great scientific and technological interest. The technological interest is mainly due to the high swelling capacity of the gels and their ability to respond to changes in the external conditions by drastic volume changes. These so-called "hydrogels" are used in applications like diapers and pharmaceutical products[1,2] and in agriculture.[3,4] The scientific interest is due to the complex interplay of counteracting forces, which determine the equilibrium swelling of the hydrogels.[5] The main contributions are the osmotic pressure from the counterions, the network elasticity, long-range electrostatic interactions, and short-range hydrophobic interactions. The delicate balance of these forces is the reason why the magnitude of the swelling and the phase behavior of polyelectrolyte gels are hard to predict.

Discontinuous volume changes for polymer gels were predicted theoretically by Dušek[6] in 1968, 10 years before they were first observed experimentally by Tanaka in 1978.[7] Tanaka found that partially hydrolyzed polyacrylamide gels in an acetone−water mixture underwent a discontinuous volume transition as a function of temperature or acetone concentration.[7,8] Later, several experimental studies have shown discontinuous or sharp continuous volume transitions when external conditions, such as temperature and solvency, were varied.[9] For example, polyelectrolyte gels containing poly(*N*-isopropylacrylamide) (pNIPAm) display a volume collapse at increasing temperature (lower critical solution temperature (LCST) behavior).[10−14] The gel collapse is attributed to the increased attraction between the network chains due to poorer solvency conditions. Sharp volume transitions of polyelectrolyte gels have also been found when replacing water with mixed solvents (e.g., ethanol/water or acetone/water) or pure organic solvent.[15] Here, the transitions are mainly attributed to the reduction of the permittivity of the solution.

To date, simulation studies on charged networks are scarce due to a combination of several factors. Evaluation of the long-range interactions in charged systems increases the simulation time substantially as compared to uncharged, otherwise equal, systems. Additionally, most of the more advanced Monte Carlo trial moves (e.g., slithering snake moves or pivot rotations), which are commonly used to accelerate the equilibration of polymer systems, are prohibited because they would disrupt the network topology. Uncharged networks have been successfully simulated by Kremer and Everaers,[16,17] Sommer,[18] and Escobedo and de Pablo.[19] Escobedo and de Pablo found discontinuous volume transitions for uncharged hydrophobic networks.[20] We have previously simulated polyelectrolyte gels possessing electrostatic, bond, and excluded-volume interactions.[21,22] A very large swelling as compared to uncharged gels was observed,[22] and the mechanism of the swelling was addressed.[21] Moreover, an assessment of different approximations used in gel theories was made. Recently, Yan and de Pablo observed a discontinuous volume transition for polyelectrolyte networks at high electrostatic coupling using a similar model.[23] Their work mainly concentrates on structural aspects. Recently, Lu and Hentschke simulated a polyelectrolyte gel with both explicit counterion and explicit solvent.[24]

In the present contribution, we used the same model as in our previous work[21,22] and include short-range attractive interactions between the polymer chains, representing the poor-solvent conditions present in many gels. We also examine the properties of the model system at reduced solvent permittivity, representing a (partial) exchange of water to organic solvents. In both cases, but for different reasons, sharp volume transitions are observed at sufficiently strong effective attraction between polymer segments, which is in close agreement with experimental data.

2. Model

The model used is basically the same as in our previous contributions[21,22] and is based on the primitive model for electrolytes. Briefly, the polyelectrolyte gel contains a charged network, counterions, and solvent. All charged species are treated explicitly as charged hard spheres, and the solvent is modeled as a dielectric continuum. The network is composed of chains connected by tetrafunctional charged cross-linkers (nodes).

* Corresponding author. E-mail: st.schneider@fz-juelich.de. Present address: Institut für Festkörperforschung, Forschungszentrum Jülich, D-52425 Jülich, Germany.

10.1021/ma035512n CCC: $27.50
Published on Web 04/22/2004

Each chain is modeled as a sequence of charged hard spheres (beads) connected by harmonic bonds. For simplicity, we use a defect-free network with a diamond-like topology, in which all the chains are of equal length. The topology of the network remains fixed; thus, the model represents a covalently cross-linked network. A short-range square-well attractive potential acting between pairs of network particles (nodes and beads) represents the hydrophobic attraction of the polymer chains. The total potential energy, U, of the system can be expressed as

$$U = U_{\mathrm{hs}} + U_{\mathrm{el}} + U_{\mathrm{bond}} + U_{\mathrm{sw}} \tag{1}$$

where the term describing the hard-sphere repulsion, U_{hs}, is given by

$$U_{\mathrm{hs}} = \sum_{i<j} u_{ij}^{\mathrm{hs}}(r_{ij}) \tag{2}$$

and

$$u_{ij}^{\mathrm{hs}}(r_{ij}) = \begin{cases} \infty, & r_{ij} < (\sigma_i + \sigma_j)/2 \\ 0, & r_{ij} \geq (\sigma_i + \sigma_j)/2 \end{cases} \tag{3}$$

with σ_i being the diameter of particle i and $r_{ij} = |\mathbf{r}_{ij}| = |\mathbf{r}_i - \mathbf{r}_j|$ the distance between the centers of particles i and j. The electrostatic potential energy, U_{el}, is given by

$$U_{\mathrm{el}} = \sum_{i<j} \frac{z_i z_j e^2}{4\pi\epsilon_0\epsilon_{\mathrm{r}}} \frac{1}{r_{ij}} \tag{4}$$

with z_i denoting the charge of particle i, e the elementary charge, ϵ_0 the permittivity of vacuum, and ϵ_{r} the relative permittivity of the solvent. The bond potential energy, U_{bond}, is given by

$$U_{\mathrm{bond}} = \sum_{m=1}^{N_{\mathrm{bond}}} \frac{k_{\mathrm{bond}}}{2} (r_{\mathrm{m,bond}} - r_0)^2 \tag{5}$$

where N_{bond} is the number of bonds in the network, $r_{\mathrm{m,bond}}$ the bond length with the equilibrium separation being $r_0 = 0.5$ nm, and the force constant $k_{\mathrm{bond}} = 0.4$ N/m. With the other interactions included, the typical root-mean-square separation between bonded beads becomes $\approx$0.55−0.60 nm. Finally, the square-well potential energy, U_{sw}, is given by

$$u_{\mathrm{sw}} = \sum_{i<j} u_{ij}^{\mathrm{sw}}(r_{ij}) \tag{6}$$

with

$$u_{ij}^{\mathrm{sw}} = \begin{cases} -\epsilon_{\mathrm{sw}}, & r_{ij} < \lambda(\sigma_i + \sigma_j)/2 \\ 0, & r_{ij} \geq \lambda(\sigma_i + \sigma_j)/2 \end{cases} \tag{7}$$

where ϵ_{sw} is the square-well depth and $\lambda(\sigma_i + \sigma_j)/2$ the square-well width. In eq 6, the sum is restricted to network particles only. In related studies, the square-well potential has been used to simulate polyion coil−globule transitions[25] and uncharged hydrophobic polymer gels.[20]

Six different polyelectrolyte gels, characterized by different short-range potentials, have been considered (see Table 1). In system 1, there is no short-range square-well attraction ($\epsilon_{\mathrm{sw}} = 0$), whereas systems 2−6

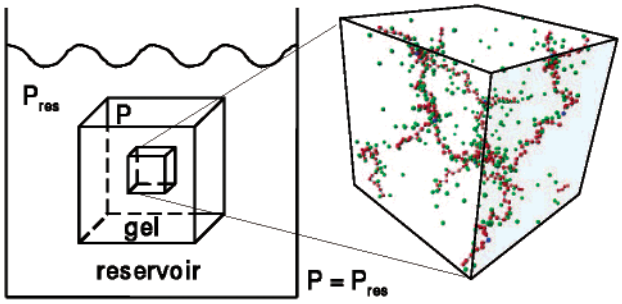

Figure 1. (left) Schematic illustration of a cubic macroscopic gel in equilibrium with a reservoir of solvent. (right) Snapshot of one unit cell of a defect-free network of diamond-like topology containing eight tetrafunctional nodes (blue spheres) linked by 16 noncrossing chains (red spheres) and 328 counterions (green spheres).

Table 1. Parameters of the Square-Well Potential of Systems Investigated

system	ϵ_{sw} [$k_{\mathrm{B}}T$]	λ	system	ϵ_{sw} [$k_{\mathrm{B}}T$]	λ
1	0	0	4	0.30	3
2	0.20	3	5	0.35	3
3	0.25	3	6	0.40	3

possess an attractive square-well interaction with increasing strength ($0 < \epsilon_{\mathrm{sw}} \leq 0.4\ k_{\mathrm{B}}T$, with k_{B} denoting the Boltzmann constant and T the temperature) and $\lambda = 3$. Furthermore, three of the systems have been investigated at different solvent permittivity. Throughout, all network particles and counterions had a diameter $\sigma_i = \sigma = 0.4$ nm and were monovalently charged $|z_i| = 1$. A single unit cell comprising 8 nodes and 16 chains, each chain composed of 20 beads, was used. The particles were enclosed in a cubic box, and periodic boundary conditions were applied. A temperature $T = 298$ K was used.

The polyelectrolyte gel is considered to be in contact with a surrounding reservoir of pure solvent, with an exchange of solvent between the gel and the reservoir. An equilibrium swelling of the gel is reached when the osmotic pressure in the gel, P, is equal to the osmotic pressure of the reservoir, P_{res} (see Figure 1). For a pure solvent, $P_{\mathrm{res}} = 0$ by definition. Throughout, the volume of the gel will be given as the reduced gel volume per particle, $V/N\sigma^3$, where N denotes the sum of node, bead, and counterion particles.

3. Simulation Methods

The Monte Carlo (MC) simulations were performed using the canonical (NVT) and isothermal−isobaric (NPT) ensembles. In the former, the number of particles, the volume of the system, and the temperature are kept constant, whereas in the latter the pressure is kept constant with a fluctuating volume.[26] The Metropolis algorithm[27] was used to generate Boltzmann-weighted configurations of the gel systems. Single particles were subjected to translational displacements, and the potential energies were calculated according to eqs 1−7. The translational displacement parameters were adjusted to the density of the gel, being 0.10 nm for the network particles and 0.15 nm for the counterions in collapsed states and larger in swollen ones. In the NPT-MC simulations, 2% of the single particle trial moves were replaced by attempted volume changes. The maximum volume change was set to ca. 0.5% of the expected equilibrium volume.The equilibration runs involved between 0.05 and 0.25 $\times$ 10^6 trial moves per particle,

and the production runs involved $0.2-1.0 \times 10^6$ trial moves per particle. The long-range electrostatic interactions were calculated using the Ewald sum.[28,29]

The reported statistical uncertainties are given as one standard deviation of the mean and were estimated by dividing the simulations into 10 sub-batches. In the NPT simulations, the correlation length of the volume fluctuations ranged from 0.7×10^3 (large volume) to 6×10^3 (small volume) trial moves per particle. The uncertainties of the reduced pressure $P\sigma^3/k_BT$ were between 0.001 and 0.03 for the simulations in the NPT ensemble and 10-fold smaller in the NVT ensemble. In the figures, error bars are given if they are larger than the size of the symbols. The uncertainties of the mean volumes from the NPT ensemble were always smaller than 3%. All simulations were carried out using the integrated Monte Carlo/molecular dynamics/Brownian dynamics simulation package Molsim.[30]

The equilibrium volumes of the polyelectrolyte gels were determined by simulations in the NPT ensemble at the external pressure $P_{res} = 0$. To assess ergodicity in these systems, simulations were started from both swollen and collapsed states. In some cases, the obtained volumes differed between the two simulations with different initial volumes, and hence one of the states was metastable, indicating discontinuous volume transitions. Partial pressure−volume isotherms were also determined from simulations in the NVT ensemble to further assess internal stability. The pressure was calculated as the sum of an ideal, a virial, and a contact term, as described earlier.[21,22]

4. Pressure−Volume Isotherms Determined from Simulations

4.1. Pressure−Volume Isotherms. Except for special approaches, simulation methods do not generally provide full pressure−volume isotherms when instabilities appear. To rationalize our findings, six different cases will be employed. Each case is defined by the shape of the isotherm and its relation to the pressure of the reservoir, $P_{res} = 0$. The discussion is, however, valid for any reservoir pressure, not necessarily zero. The six different isotherms (solid curves) in conjunction with the $P_{res} = 0$ function (dotted line) schematically shown in Figure 2 represent the different situations, in the following referred to as cases I−VI.

In case I, the pressure decreases monotonically as the volume is increased. No phase transition appears, and the intersection point of the isotherm with the $P = P_{res}$ line gives the volume of the system in equilibrium with the reservoir.

In cases II−VI, all isotherms show a so-called van der Waals loop with instabilities ($\partial P/\partial V > 0$) at intermediate volumes. For a macroscopic system, the pressure does not follow the loop. Instead, a phase separation appears, at which the pressure is constant until the phase transition (e.g., from the collapsed to the swollen gel) is completed. The transition pressure (P^*) can be constructed by the so-called "Maxwell-" or "equal-area-construction", where a constant pressure line (thin solid lines in Figure 2) is drawn such that the two areas enclosed by the loop and the line are equal.[31] Depending on the value of P^* and on the number of intersections with the $P = P_{res}$ line, this set of five cases can further be distinguished.

Case II is characterized by $P^* > P_{res}$ and only one intersection point with the $P = P_{res}$ line (filled circle).

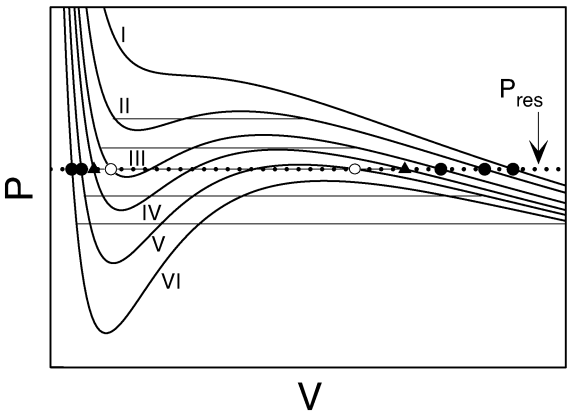

Figure 2. Schematic representation of six pressure−volume isotherms (solid curves) and an external pressure line P_{res} (dotted line), representing six cases characterized by the shape of the isotherms and their relations to the pressure P_{res}. In cases II−VI, discontinuous volume transitions appear at the transition pressures P^* given by the equal-area constructions (thin solid lines). In cases I−III, V, and VI, the volumes of the equilibrium states (filled circles) and the metastable states, if present (open circles), are given, and in case IV, the volumes of the two coexisting states (filled triangles) at $P = P_{res}$ are given.

In case III, again $P^* > P$, but now the isotherm intersects the $P = P_{res}$ line three times. The large-volume intersection (filled circle) represents the equilibrium state, the small-volume one (open circle) corresponds to a metastable state, and the intermediate-volume intersection corresponds to an unstable state. In case IV, $P^* = P_{res}$, and a coexistence between the collapsed and the swollen states (filled triangles) appears. In case V (as for cases III and IV), the isotherm intersects the $P = P_{res}$ line three times, but now $P^* < P_{res}$. This results in a stable collapsed gel (filled circle) and a metastable swollen gel (open circle). Finally, case VI is characterized by only one intersection with the $P = P_{res}$ line, appearing at a small volume (filled circle) and corresponding to a collapsed gel.

4.2. NPT Ensemble. Assume that simulations in the NPT ensemble are performed at $P = P_{res}$ and, moreover, that large and small initial volumes are used. Simulations resulting in cases I, II, or VI would unambiguously provide correct equilibrium volumes, independently of the initial volume. However, in case III or V, two different volumes could be obtained. For example, in case III, the system might be trapped in a metastable state if the initial volume was sufficiently small. The probability of finding metastable states depends on the relation of the free energy barrier between the metastable and stable states and the pressure−volume fluctuations. In practice, such metastable states were always observed when expected. Finally, in case IV with $P = P_{res}$, we expect simulations starting with large and small initial volumes always to provide the volume of the two coexisting states at the pressure P_{res}.

4.3. NVT Ensemble. As compared to simulations in the NPT ensemble, a more detailed picture of the pressure−volume relations can be obtained using the NVT ensemble. From such simulations, the two complete state branches with $\partial P/\partial V < 0$, representing all stable and metastable states, can be determined. (In NPT simulations, metastable states are not guaranteed to be found.) However, no meaningful pressures can be obtained for the unstable region (large interfacial effects), impeding a correct Maxwell construction and the

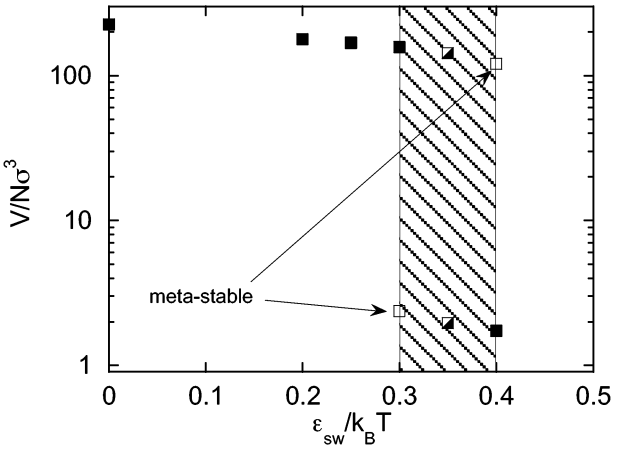

Figure 3. Reduced gel volume per particle, $V/N\sigma^3$, as a function of the square-well depth, ϵ_{sw}, at $\lambda = 3$ and $\epsilon_r = 80$, obtained from NPT-MC simulations at $P_{res} = 0$, starting from swollen and collapsed states. Filled symbols denote stable states, and open symbols denote metastable states. Half-filled symbols are used, if it was not possible to determine whether a state was stable or metastable. The shaded area shows the range of ϵ_{sw} where a discontinuous volume transition is expected.

Table 2. Reduced Gel Volume per Particle, $V/N\sigma^3$, of Equilibrium and Metastable States, Obtained from NPT Simulations at Zero Pressure and $\epsilon_r = 80$; Volumes of the Metastable States Are Given in Parentheses

system 1	system 2	system 3	system 4	system 5[a]	system 6
226 ± 1	179 ± 4	167 ± 2	158 ± 1 (2.35 ± 0.02)	143 ± 2 1.95 ± 0.01	1.74 ± 0.01 (120 ± 2)

[a] The distinction of equilibrium and metastable states could not be made; see text.

determination of the transition pressure. Nevertheless, in most cases $|P^* - P_{res}| \gg 0$, and an approximate determination of P^* is sufficient to evaluate the sign of $(P^* - P_{res})$. Hence, conditions at which the discontinuous volume transitions appear at the pressure P_{res} can be determined fairly accurately.

5. Results and Discussion

5.1. Variable Square-Well Potential Depth at Constant Solvent Permittivity. The effect of the solvency conditions on the gel swelling was investigated at the relative permittivity $\epsilon_r = 80$ by varying the depth of the attractive square-well potential. For comparison, the interaction strength that results in Θ-conditions for an uncharged single chain was determined to be $\epsilon_{sw} \approx 0.04\ k_BT$. Simulations in the NPT ensemble, starting from both swollen and collapsed states, and in the NVT ensemble were performed.

NPT Ensemble. Figure 3 shows the reduced gel volume per particle as a function of the depth of the square-well potential for systems 1−6 at $P_{res} = 0$, as obtained from the NPT-MC simulations starting from swollen and collapsed states, respectively. The corresponding numerical values are reported in Table 2.

For the three lower ϵ_{sw} (systems 1−3), the volumes obtained were independent of the initial volumes, indicating that the results represent gel volumes at equilibrium. For potential depths, ϵ_{sw}, between 0.3 and 0.4 k_BT (systems 4−6), however, volumes differing by a factor of approximately 70 were obtained, depending on the initial volumes. From the NPT simulations at the single pressure $P_{res} = 0$ alone, discrimination into stable and metastable states cannot be made.

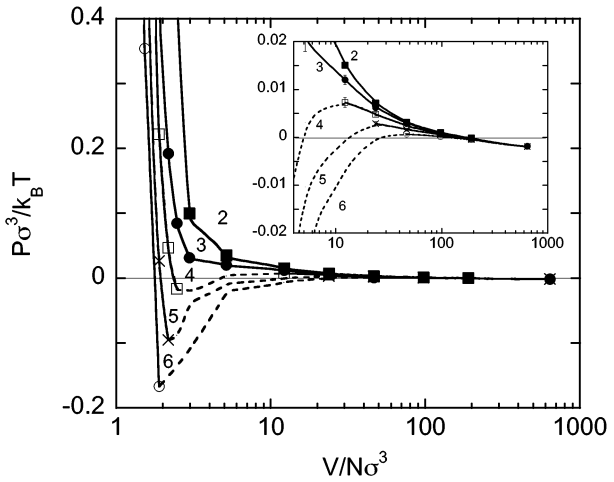

Figure 4. Reduced pressure, $P\sigma^3/k_BT$, as a function of the reduced gel volume per particle, $V/N\sigma^3$, obtained from NVT-MC simulations, for the square-well depths $\epsilon_{sw} = 0.20\ k_BT$ (filled squares), 0.25 k_BT (filled circles), 0.30 k_BT (open squares), 0.35 k_BT (crosses), and 0.40 k_BT (open circles) at $\lambda = 3$ and $\epsilon_r = 80$. Solid curves represent the pressure−volume isotherms under stable and locally stable conditions, corresponding to $\partial P/\partial V < 0$, whereas dashed curves schematically indicate van der Waals loops (just a guide to the eye) under unstable conditions. For each system, the instability region was assumed to extend between volumes V_1 and V_2 for which $P_1 < P_2$ was observed. The inset is an expansion at pressures near zero.

NVT Ensemble. The corresponding $P(V)$ isotherms obtained from NVT-MC simulations are given in Figure 4. The symbols denote pressures obtained at a given volume, and the solid curves join the data and represent stable conditions ($\partial P/\partial V < 0$), whereas the dashed curves schematically indicate unstable conditions.

For the two weakest nonzero short-range attractive interactions (systems 2 and 3), the isotherms are monotonic (case I) and no phase transition is present. The single points of intersection with the $P_{res} = 0$ line give the equilibrium volumes (see inset of Figure 4).

For the stronger interactions (systems 4−6), the isotherms show a nonmonotonic behavior, demonstrating phase instability. The curves intersect the $P_{res} = 0$ line three times, and hence the gels possess two, at least locally, stable states when in equilibrium with a reservoir of pure solvent. For the reasons mentioned above, it is not possible to determine the transition pressure P^* accurately. Nevertheless, for $\epsilon_{sw} = 0.30\ k_BT$ (system 4), P^* is likely to be positive (note the logarithmic volume scale) (case III), implying a swollen equilibrium state and a collapsed metastable state at $P_{res} = 0$. Similarly, for $\epsilon_{sw} = 0.40\ k_BT$ (system 6) the pressure exceeds zero only slightly at large volumes, so it can be argued that P^* is negative (type VI). Thus, for system 6 at $P_{res} = 0$, the collapsed state should be the equilibrium one. However, for the intermediate interaction strength, $\epsilon_{sw} = 0.35\ k_BT$ (system 5), it is not possible to draw similar conclusions. Hence, the first-order volume transition should appear for ϵ_{sw} between 0.3 and 0.4 k_BT. The shaded area in Figure 4 indicates this interval.

A comparison between the data from the NPT and NVT simulations shows that the results at the equilibrium and metastable states from the two ensembles are in very good agreement with each other. Taking the equilibrium volume ($P = 0$) of system 2 as an example of a swollen state, the NPT simulations gave $V/N\sigma^3 = 179 \pm 4$. The pressure calculated in an NVT simulation

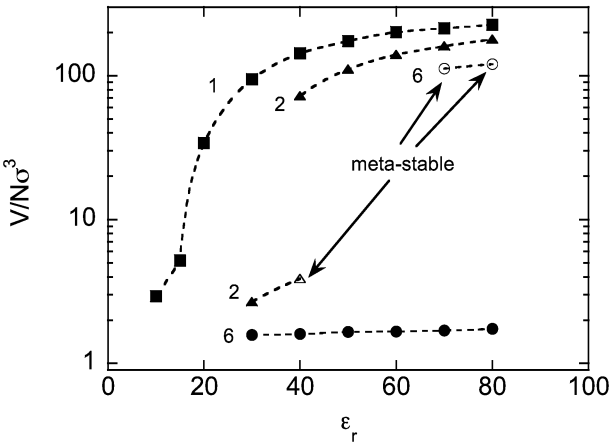

Figure 5. Reduced gel volume per particle, $V/N\sigma^3$, as a function of the relative permittivity, ϵ_r, for the square-well depths $\epsilon_{sw} = 0.0\ k_BT$ (system 1, squares), $0.2\ k_BT$ (system 2, triangles), and $0.4\ k_BT$ (system 6, circles) at $\lambda = 3$, obtained from NPT-MC simulations. Filled symbols denote stable states and open symbols denote metastable states.

Table 3. Reduced Gel Volume per Particle, $V/N\sigma^3$, of Equilibrium and Metastable States, Obtained from NPT Simulations at Zero Pressure and Variable Relative Permittivities; Volumes of the Metastable States Are Given in Parentheses

ϵ_r	system 1	system 2	system 6
10	2.93 ± 0.02		
15	5.18 ± 0.05		
20	34.0 ± 0.7	1.48 ± 0.01	
30	95 ± 2	2.68 ± 0.02	1.58 ± 0.01
40	143 ± 1	(3.9 ± 0.2) 72 ± 2	1.60 ± 0.01
50	174 ± 3	111 ± 2	1.65 ± 0.01
60	201 ± 2	140 ± 3	1.67 ± 0.01
70	214 ± 3	156 ± 3	1.69 ± 0.01 (112 ± 2)
80	226 ± 1	179 ± 4	1.74 ± 0.01 (120 ± 2)

at the same density was $P\sigma^3/k_BT = 0.0002$. Furthermore, similar comparison of the collapsed state of system 6 gave $V/N\sigma^3 = 1.74 \pm 0.01$ (NPT ensemble) and $P\sigma^3/k_BT = 0.003$ (NVT ensemble) at the same density. The pressures calculated from the NVT simulations are indeed very close to zero (cf. Figure 4).

To conclude, when in equilibrium with a reservoir characterized by $\epsilon_r = 80$ and $P_{res} = 0$, the polyelectrolyte gel undergoes a discontinuous volume transition from a swollen to a collapsed state for some ϵ_{sw} in the interval $0.3-0.4\ k_BT$ as the short-range interaction strength is increased.

5.2. Variable Solvent Permittivity. The swelling behavior of polyelectrolyte gels with no (system 1), weak (system 2), and strong (system 6) short-range square-well attractive potentials was investigated at dielectric permittivities $\epsilon_r = 80$ and smaller. As for the examination of the square-well potential depth, both NPT and NVT ensembles were used. Figure 5 shows the reduced gel volume per particle for the three systems as a function of the relative permittivity of the solvent at zero pressure, with the corresponding numerical data compiled in Table 3. The $P(V)$ isotherms at selected relative permittivities obtained from the NVT simulations are displayed in Figure 6.

No Square-Well Attraction. The swelling behavior of system 1 is displayed by the top curve (filled squares) of Figure 5. Starting from a high relative permittivity, the equilibrium volume is $V/N\sigma^3 \approx 200$ and decreases slowly to $V/N\sigma^3 \approx 100$ at $\epsilon_r = 30$. Between $\epsilon_r = 30$ and 15, the equilibrium volume reduces drastically and becomes $V/N\sigma^3 = 5.18$ (or $V/N_{network}\sigma^3 = 10.36$) at $\epsilon_r = 15$. At even smaller ϵ_r, the volume reduction levels out. The equilibrium volume per network particle of the corresponding uncharged network was previously determined to be $18\sigma^3$.[22] Hence, at $\epsilon_r = 15$ the net effect of the electrostatic interaction is a 2-fold contraction of the gel. Khokhlov and Kramerenko called this state, which was more collapsed than the corresponding uncharged gel, the "supercollapsed" state.[32]

In Figure 6a, the isotherms for system 1 at $\epsilon_r = 10$, 15, and 20 are shown. For $\epsilon_r = 20$, no instability is present (case I). The gel in equilibrium with the solvent is still fairly swollen, $V/N\sigma^3 = 34.0$, but its volume has decreased as compared to larger ϵ_r. Shifting to $\epsilon_r = 15$ results in a small instability with a negative transition pressure (case VI). Under these conditions, the gel volume is small, $V/N\sigma^3 = 5.18$. At even lower permittivity $\epsilon_r = 10$, the instability becomes more pronounced, and the gel volume decreases further.

At large permittivity, the equilibrium volume is to a large degree governed by the competition between the osmotic pressure of the counterions and the network elasticity. When the electrostatic interactions become stronger as ϵ_r is reduced, the counterions are more strongly attracted to the charged polymer chain, and hence their contribution to the osmotic pressure decreases. To illustrate the increasing counterion condensation with decreasing solvent permittivity, the bead−counterion radial distribution functions for three different permittivities are shown in Figure 7. At some point, the osmotic pressure of the counterions becomes so attenuated that the large swelling, originally induced by it and balanced by the network elasticity, vanishes. At this stage, the gel volume becomes close to that of an uncharged gel. At an even larger electrostatic coupling, the cohesiveness of the electrostatic interaction, originating from spatial charge correlations, actually reduces the gel volume further. Previous simulations have examined the contraction of single polyions with counterions upon an increase of the electrostatic coupling.[33−35] The attractive interactions between polymer chains, which lead to the "supercollapsed" state, might have an even larger influence on the swelling behavior of charged networks than what is discussed here. Khokhlov and Kramerenko suggest that the relative dielectric constant inside a polymer gel depends on the polymer volume fraction.[32] This implies a decrease of the permittivity with a decrease of the gel volume. This effect is not included in this study but would presumably lead to a shift of the volume transition to larger permittivities of the solvent.

Weak Short-Range Attraction. With a weak short-range chain interaction, $\epsilon_{sw} = 0.2\ k_BT$ (system 2), the volume transition shifts to higher ϵ_r, as can be seen in 5. At the sharp collapse occurring at $\epsilon_r \approx 30-40$, the gel volume decreases 50-fold. At $\epsilon_r = 40$, a metastable collapsed state was obtained.

In Figure 6b, the isotherms for system 2 are given at $\epsilon_r = 30$, 40, 50, and 80. At $\epsilon_r = 80$ and 50, no phase transition can be observed at any pressure (case I). The isotherm at $\epsilon_r = 30$ displays a negative transition pressure (case VI). Finally, the volume transition at $\epsilon_r = 40$ occurs most likely at a positive pressure (case III), which leaves us with a swollen equilibrium state and a

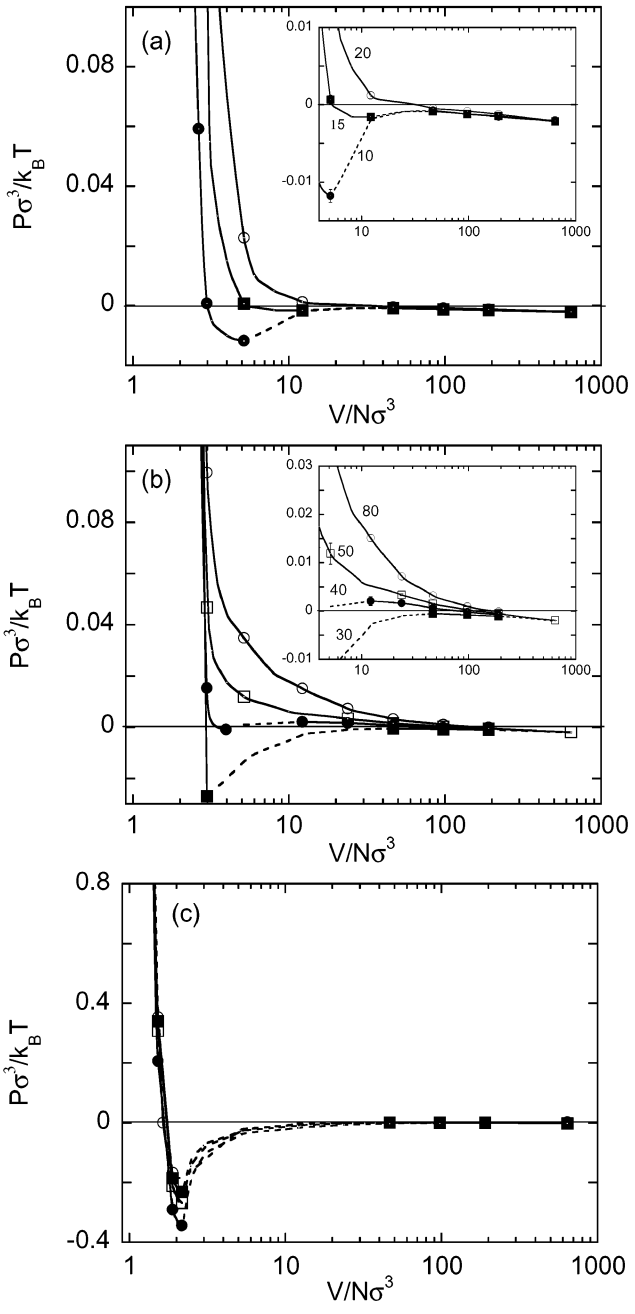

Figure 6. Reduced pressure, $P\sigma^3/k_BT$, as a function of the reduced gel volume per particle, $V/N\sigma^3$, for (a) $\epsilon_r = 10$ (filled circles), 15 (filled squares), and 20 (open circles) at $\epsilon_{sw} = 0$ (system 1), (b) $\epsilon_r = 30$ (filled squares), 40 (filled circles), 50 (open squares), and 80 (open circles) at $\epsilon_{sw} = 0.20\ k_BT$ (system 2), and (c) $\epsilon_r = 40$ (filled circles), 60 (open squares), 70 (filled squares), and 80 (open circles) at $\epsilon_{sw} = 0.40\ k_BT$ (system 6), from NVT-MC simulations. Solid and dashed curves have the same meaning as in Figure 4. The insets are expansions at pressures near zero.

collapsed metastable state at $P = 0$. Thus, a sharp volume transition appears for a relative permittivity between 30 and 40.

Snapshots of the polyelectrolyte gels at $\epsilon_r = 30$ and 40 are provided in Figure 8. A comparison of the two snapshots illustrates the large difference of the densities at the two permittivities. In the collapsed state, the total volume fraction of all particles is 0.20, and the molar bead concentration becomes 4.8 M. The network beads and counterions are strongly mixed, and the situation resembles a concentrated electrolyte solution. In the

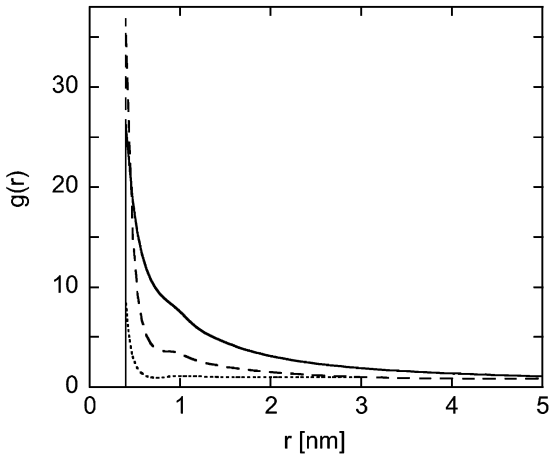

Figure 7. Bead−counterion radial distribution functions for systems without square-well attraction (system 1) with $\epsilon_r = 80$ (solid curve), $\epsilon_r = 20$ (dashed curve), and $\epsilon_r = 15$ (dotted curve) at $P\sigma^3/k_BT = 0$. Note that the densities are different at the three different conditions (see Table 3).

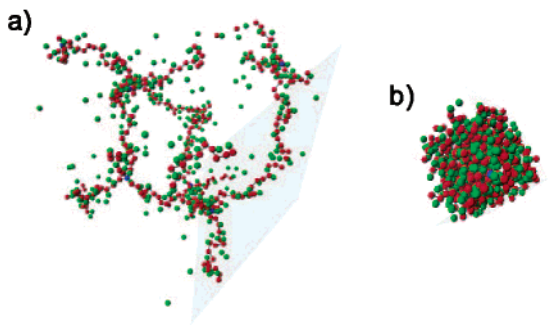

Figure 8. Snapshots of polyelectrolyte gels from simulations for (a) $\epsilon_r = 40$ and (b) $\epsilon_r = 30$ at $\epsilon_{sw} = 0.2\ k_BT$ and $\lambda = 3$ (system 2). The pictures are drawn to scale.

swollen state, the chains are strongly stretched, and most of the counterions are accumulated near the network beads. Large regions with very few counterions appear between the chains.

Strong Short-Range Attraction. Figure 5 shows that an increase of the depth of the square-well potential to 0.4 k_BT (system 6) results in a collapsed gel with an equilibrium volume per particle of $\approx 1.6\sigma^3$ over the whole range of relative permittivity investigated. For $\epsilon_r \leq 60$ only collapsed states were found from NPT simulations, independent of the initial volume. For $\epsilon_r = 70$ and 80, swollen metastable states were observed when starting from a swollen system. The volumes of these metastable states are $\approx$100 times larger than the volumes of the collapsed equilibrium states.

Figure 6c shows that the swollen and the collapsed states are in equilibrium with each other at negative transition pressures ($P^* < 0$). At high relative permittivity ($\epsilon_r = 70$ and 80), the van der Waals loops intersect with the $P_{res} = 0$ line (case V), and in addition to the stable collapsed states, metastable swollen states are present. At $\epsilon_r = 60$, the complete loop appears at negative pressure (case VI), which completes the motivation of the classification made in Figure 6.

6. Conclusion

The swelling behavior of polyelectrolyte gels with short-range attractive square-well potential and/or at low relative permittivity of the solution was investigated

by Monte Carlo simulations. A simple square-well potential was introduced to represent an attractive interaction that is present in many gel systems at elevated temperature. A change of the relative permittivity was used to represent the use of organic solvents.

The pressure−volume isotherms for polyelectrolyte gels with a short-range attraction between chain beads show regions of instability at realistic values of the square-well potential. This demonstrates the occurrence of a first-order volume transition where swollen and collapsed gels coexist. Consequently, very large changes of the equilibrium volume appear at a critical value of the short-range attraction. The results are consistent with experimental observations where similar abrupt volume changes appear with increasing temperature due to concomitant deterioration of the solvency conditions.[8,7,12,13]

Pressure−volume instabilities also appear for charged gels without additional short-range attraction upon a reduction of the permittivity of the solution, and at the critical relative permittivity $\epsilon_r \approx 20$, the swollen gel undergoes a strong contraction. Below the transition, the gel volume is smaller than for the corresponding uncharged gel. For polyelectrolyte gels with a short-range attraction, the critical relative permittivity increases as the short-range attraction becomes stronger.

Experimentally, as well as in the present model study, the volume transitions, which appear at critical short-range attraction and at the critical permittivity, display the common feature of a 10−100-fold reduction of the gel volume at a small variation of the conditions. However, the origin of the collapse is different. In the first case, the collapse is driven by an attraction between beads of the network. At some stage, when the short-range attraction is increased, the balance between (i) the collapsed state favored by chains and (ii) the swollen state favored by the counterion entropy is shifted to the collapsed one. In the case of permittivity variation, the role of the electrostatic interaction is changed through a change of the enthalpy−entropy balance. The contribution to the osmotic pressure from the small ions is reduced as the electrostatic coupling is increased, and eventually the collapsed and energy dominated state appears. Similar discontinuous transition appears in solution of polyelectrolyte at sufficient electrostatic coupling.

Acknowledgment. We thank Sergei Gavryushov for his contributions during initial stages of this work and the Centre for Amphiphilic Polymers from Renewable Resources (CAP) for financial support.

References and Notes

(1) Eichenbaum, G. M.; Kiser, P. F.; Dobrynin, A. V.; Simon, S. A.; Needham, D. *Macromolecules* **1999**, *32*, 4867.
(2) Peppas, N. A.; Bures, P.; Leobandung, W.; Ichikawa, H. *Biopharm.* **2000**, *50*, 27.
(3) Kazanskii, K. S.; Dubrovskii, S. A. *Adv. Polym. Sci.* **1992**, *104*, 97.
(4) Rudzinski, W. E.; Dave, A. M.; Vaishnav, U. H.; Kumbar, S.; Kulkami, A. R.; Aminabhavi, T. M. *Design Monom. Polym.* **2002**, *5*, 39.
(5) Khokhlov, A. R.; Starodubtzev, S. G.; Vasilevskaya, V. V. In *Responsive Gels: Volume Transitions I*; Vol. 109 of *Adv. Polym. Sci.;* Dušek, K., Ed.; Springer-Verlag: New York, 1993.
(6) Dušek, K.; Patterson, D. *J. Polym. Sci., Part A2* **1968**, *6*, 1209.
(7) Tanaka, T. *Phys. Rev. Lett.* **1978**, *40*, 820.
(8) Tanaka, T.; Fillmore, D.; Sun, S.-T.; Nishio, I.; Swislow, G.; Shah, A. *Phys. Rev. Lett.* **1980**, *45*, 1636.
(9) *Adv. Polym. Sci.* Vols. 109 and 110; Dušek, K., Ed.; Springer-Verlag: New York, 1993.
(10) Matsuo, E. S.; Tanaka, T. *J. Chem. Phys.* **1988**, *89*, 1695.
(11) Kawasaki, H.; Sasaki, S.; Maeda, H. *J. Phys. Chem. B* **1997**, *101*, 4184.
(12) Kokufuta, E.; Wang, B.; Yoshida, R.; Khokhlov, A. R.; Hirata, M. *Macromolecules* **1998**, *31*, 6878.
(13) Kokufuta, E. In *Physical Chemistry of Polyelectrolytes*; Radeva, T., Ed.; Marcel Dekker: New York, 2001.
(14) Ogawa, K.; Ogawa, Y.; Kokufuta, E. *Colloids Surf. A* **2002**, *209*, 267.
(15) Amiya, T.; Tanaka, T. *Macromolecules* **1987**, *20*, 1162.
(16) Everaers, R.; Kremer, K. *Macromolecules* **1995**, *28*, 7291.
(17) Everaers, R.; Kremer, K. *Phys. Rev. E* **1996**, *53*, R37.
(18) Sommer, J. U.; Schulz, M.; Trautenberg, H. L. *J. Chem. Phys.* **1993**, *98*, 7515.
(19) Escobedo, F. A.; de Pablo, J. J. *Phys. Rep.—Rev. Sect. Phys. Lett.* **1999**, *318*, 85.
(20) Escobedo, F. A., de Pablo, J. J. *Mol. Phys.* **1997**, *90*, 437.
(21) Schneider, S.; Linse, P. *Eur. Phys. J. E* **2002**, *8*, 457.
(22) Schneider, S.; Linse, P. *J. Phys. Chem. B* **2003**, *107*, 8030.
(23) Yan, Q.; de Pablo, J. J. *Phys. Rev. Lett.* **2003**, *91*, 018301-1.
(24) Lu, Z.-Y.; Hentschke, R. *Phys. Rev. E* **2003**, *67*, 061803-1.
(25) Khan, M. O.; Mel'nikov, S. M.; Jönsson, B. *Macromolecules* **1999**, *32*, 8836.
(26) Allen, M. P.; Tildesley, D. J. *Computer Simulation of Liquids*; Oxford University Press: Oxford, 1989.
(27) Metropolis, N.; Rosenbluth, A. W.; Rosenbluth, M. N.; Teller, A. H.; Teller, E. *J. Chem. Phys.* **1953**, *21*, 1087.
(28) Ewald, P. P. *Ann. Phys.* **1921**, *64*, 253.
(29) Lobaskin, V.; Linse, P. *J. Chem. Phys.* **1998**, *109*, 3530.
(30) Linse, P. MOLSIM 3.4. Lund University, Lund, 2003.
(31) Atkins, P. W. *Physical Chemistry*, 6th ed., Oxford University Press: Oxford, 1994.
(32) Khokhlov, A. R.; Kramerenko, E. Yu. *Macromolecules* **1996**, *29*, 681.
(33) Winkler, R. G.; Gold, M.; Reineker, P. *Phys. Rev. Lett.* **1998**, *80*, 3731.
(34) Mel′nikov, S. M.; Khan, M. O.; Lindman, B.; Jönsson, B. *J. Am. Chem. Soc.* **1999**, *121*, 1130.
(35) Pais, A. A. C. C.; Miguel, M. G.; Linse, P.; Lindman, B. *J. Chem. Phys.* **2002**, *117*, 1385.

MA035512N